Journal of Photochemistry and Photobiology A: Chemistry 226 (2011) 36–41

Contents lists available at SciVerse ScienceDirect

Journal of Photochemistry and Photobiology A: Chemistry

journal homepage: www.elsevier.com/locate/jphotochem

Visible light-induced hydrogen production from glycerol aqueous solution on hybrid Pt–CdS–TiO_2 photocatalysts

Marcos de Oliveira Melo[a], Luciana Almeida Silva[a,b,*]

[a] Instituto de Química, Universidade Federal da Bahia, Campus de Ondina, Salvador 40170-290, Bahia, Brazil
[b] Instituto Nacional de Ciência e Tecnologia, INCT, de Energia e Ambiente, Universidade Federal da Bahia, 40170-290 Salvador, Bahia, Brazil

ARTICLE INFO

Article history:
Received 10 March 2011
Received in revised form 4 October 2011
Accepted 11 October 2011
Available online 19 October 2011

Keywords:
Hydrogen
Glycerol
Visible light
Photoinduced reforming
Photocatalysis

ABSTRACT

Binary (Pt/hex-CdS) and ternary (Pt/CdS/TiO_2 and Pt/TiO_2/hex-CdS) hybrid photocatalysts were evaluated in photoinduced reforming of glycerol under visible light irradiation ($\lambda > 418$ nm). The resulting hybrid materials are photocatalytically efficient with respect to hydrogen gas production. The relative order of reactivity for the synthesized hybrid catalysts was found to be: Pt/hex-CdS > Pt/CdS/TiO_2 > Pt/TiO_2/hex-CdS. The systems with CdS/aqueous solution interfacial contact showed higher activity, suggesting that the hydrogen production mechanism can be strongly influenced by hydrolytic surface reactions on CdS. The potential gradient created at the CdS/TiO_2 or TiO_2/hex-CdS interface may also play an important role in the photoelectrochemical mechanism. Therefore, carbonyl compounds such as acrolein and propanone, identified in the liquid phase after 7 h of irradiation, lead us to propose the first steps of a photoelectrochemical mechanism in the photoinduced reforming of glycerol.

1. Introduction

Hydrogen is a storable, clean, and environmentally friendly fuel whose combustion results in the generation solely of water, with no emissions of atmospheric pollutants, greenhouse gases or particulates. However, about 95% of hydrogen currently derives from fossil fuels, mainly by steam reforming of natural gas and petroleum, while the remaining 5% comes from the electrolysis of water. Because this process involves the use of nonrenewable resources or high energy consumption, this form of hydrogen production is not sustainable or economically feasible. On the other hand, the increasing global demand for biofuels has created many production-related problems; one example is biodiesel, which generates huge quantities of glycerol as a by-product [1]. Over the last few years, several research groups have focused on devising innovative solutions to give an appropriate destination to excessive glycerol production. Glycerol has been used to produce hydrogen from different methods such as steam reforming [2], gasification [3], autothermal reforming [4], aqueous-phase reforming [5], electrochemical reforming [6], photofermentation [7] and supercritical water reforming [8] processes. The majority of studies on hydrogen production from glycerol have focused on thermochemical routes. However, hydrogen can be produced from biomass in ambient conditions (temperature and pressure) via a photocatalytic route, an efficient, ecologically benign and low-cost process. This technology is based on photoelectrochemical cells operating with two redox systems [9–18].

Semiconductor-mediated photocatalytic processes have been widely investigated in recent years as potentially efficient, economic and environmentally friendly methods for a wide range of industrial applications, including mineralization of organic pollutants and disinfection of water and air [18–23]. Many works [24–30] have shown that the photocatalytic degradation of organic compounds such as azo dyes, proteins, alcohols, sugars, and organic acids can take place with simultaneous production of hydrogen over irradiated semiconductor photocatalyst suspensions. The production of hydrogen and oxygen by water cleavage takes place under non-aerated conditions and is achieved by photogenerated electrons and holes, respectively, provided their energy suffices to reduce protons toward hydrogen molecules and to oxidize water toward oxygen. On the other hand, the photocatalytic oxidation of organic compounds takes place in the presence of oxygen with the participation of photogenerated holes, which act either directly or indirectly by generating hydroxyl radicals ($OH^{\bullet}$), finally leading to the production of CO_2 and H_2O. In this case, photogenerated electrons are consumed by chemisorbed oxygen to form superoxide radicals ($O_2^{-\bullet}$). In a photoinduced reforming process, the two reactions are combined, i.e., the photocatalytic treatment of aqueous solutions of biomass components and derivatives takes place under non-aerated conditions. This results in the oxidation of the organic substrate by holes toward CO_2, which is accompanied by production of gas-phase hydrogen from water, while the

* Corresponding author at: Instituto de Química, Universidade Federal da Bahia, Campus de Ondina, Salvador 40170-290, Bahia, Brazil. Tel.: +55 71 3283 6881.
E-mail address: las@ufba.br (L.A. Silva).

1010-6030/$ – see front matter © 2011 Elsevier B.V. All rights reserved.
doi:10.1016/j.jphotochem.2011.10.012

oxidation of water reaction and the formation of superoxide radicals are suppressed.

Kondarides et al. [31] tested a large variety of biomass-derived components, including monosaccharides such as pentoses (ribose, arabinose) and hexoses (glucose, galactose, fructose, and mannose), alcohols (methanol, ethanol, propanol, and butanol) and organic acids (acetic acid, formic acid). In all these cases, the amounts of H_2 and CO_2 produced were found to be in accordance to the stoichiometry of the following general reforming reaction:

$$C_xH_yO_z + (2x - z)H_2O \rightarrow xCO_2 + (2x - z + y/2) \quad H_2 \qquad (1)$$

Few studies have focused on the photocatalytic reforming of glycerol. The work published by Daskalaki and Kondarides [32] investigated the photoreforming of glycerol with the use of Pt/TiO_2 photocatalyst under UV light irradiation. Their results indicated that hydrogen can be produced efficiently by photocatalytic reforming of aqueous solutions of glycerol, eventually leading to the complete conversion of glycerol into H_2 and CO_2.

The main researches into hydrogen production by photoinduced reforming of biomass derivatives have focused on the TiO_2 photocatalyst. However, the major drawback of TiO_2 is its inability to utilize the visible light due to its wide band gap at 3.2 eV, which corresponds to a wavelength in the UV region. Sunlight is known to contain only about 3% of UV light. So far, research efforts have focused mainly on extending the photosensitivity of semiconductor photocatalysts toward the visible light region in order to fully harvest solar energy, since it accounts for approximately 43% of the incoming solar energy spectrum. Currently, the major challenge in this field is the discovery of a photocatalyst that is able to drive the photoinduced reformation of biomass derivatives under visible light irradiation.

CdS, an n-type semiconductor with a band gap energy of 2.4 eV, has been shown to have photocatalytic activity for hydrogen production under visible light irradiation in the presence of alcohols such as ethanol and isopropanol [25,33]. However, the hydrogen production rate with CdS powder has proved to vary considerably. The hexagonal crystal structure (wurtzite) prevails in materials that exhibit high efficiency, while the cubic crystal structure prevails in those that are not efficient [34]. An alternative method to improve the photoefficiency of CdS is by hybridization with metal oxides such as TiO_2. Nano-sized TiO_2 particles deposited on bulk CdS with a higher efficiency hexagonal phase CdS have demonstrated a high rate of hydrogen production under visible light from water containing sulfide and sulfite as sacrificial reagents [35,36]. The superior activity of the composite photocatalyst is believed to be due to faster charge separation compared to CdS alone upon initial light absorption, caused by the rapid diffusion of photoelectrons generated in bulk CdS toward surrounding TiO_2 nanoparticles. On the other hand, nano-sized CdS and TiO_2 particles can be combined to obtain a composite with a large surface area. In this case, TiO_2 plays a dual role in the hybrid: it supports and prevents the aggregation of CdS, and enhances the charge separation by forming a potential gradient at the interface of CdS and TiO_2, which increases the photocatalytic efficiency [37]. In an attempt to find a highly efficient photocatalyst for the photoinduced reforming of glycerol under visible light irradiation for purposes of hydrogen production, we have evaluated the series of hybrid CdS and TiO_2 catalytic systems and pure hexagonal phase CdS in the photocatalytic treatment of aqueous glycerol solutions.

2. Experimental

2.1. Photocatalysts preparation

Bulk-phase, hex-CdS (dubbed sample 1) was synthesized by heat-treating commercial-grade CdS (Aldrich, yellow powders) at 700 °C under a nitrogen flow for 1 h [25]. The nanocomposite photocatalysts, TiO_2/hex-CdS (dubbed sample 2) and CdS/TiO_2 (dubbed sample 3), were prepared by two different procedures. In the first procedure, the hexagonal CdS was stirred in isopropyl alcohol and titanium isopropoxide (in a mole ratio of Ti to CdS of 4) and water was added dropwise. The prepared composite powder, TiO_2/hex-CdS was filtered, dried, and calcined at 400 °C for 2 h under air [35]. In the second procedure, the nano-sized CdS was deposited on the surface of the base substrate by direct reactions between $CdCl_2$ and thiourea in an ammonia bath (NH_4OH, 14.4 M) at 85 °C for 1 h in a solution containing the appropriate amount of dispersed TiO_2-P25 [38]. The product, CdS/TiO_2, was subsequently washed with acetone, water, and finally with absolute ethanol and dried overnight at 110 °C. The sample was then dried at 400 °C for 1 h.

All the samples were platinized using typical photodeposition method which consisted of adding the appropriate amount of 8% $H_2PtCl_6{\cdot}6H_2O$ solution *in situ* during the photoreaction tests.

2.2. Characterization

The powders were characterized by X-ray diffraction (Shimadzu XRD6000), using Cu Kα, Ni-filtered radiation, and a scan rate of $2^\circ\ 2\theta\ min^{-1}$, in a 2θ range of 5–80°, at 35 kV and 15 mA.

The photoacoustic (PA) experiments were performed using a spectrophotometer equipped with a 1000 W xenon arc lamp whose beam was modulated by a variable-speed chopper (SRS, model SR540). A monochromator was used in combination with appropriate absorption filters to eliminate order effects for wavelength selection (400–900 nm). The monochromator output beam was then directed into a conventional PA cell in which a 1/2 in. diameter condenser microphone (Bruel and Kjaer, model 4165) is mounted on one of the walls. The microphone signal was pre-amplified and fed to a lock-in amplifier (SRS, model SR830). The spectra were stored in a microcomputer connected to the lock-in amplifier.

2.3. Photocatalytic reactions

A high-pressure 500 W Hg–Xe arc lamp was used as the light source for the photocatalytic reactions. The collimated light beam was passed through an IR filter, a focusing lens and a 418 nm cutoff filter before reaching the photocatalytic cell, which was air cooled to maintain a constant temperature. Since it is well known that colloidal CdS suspensions undergo photocorrosion and photocatalytic dissolution under oxidant conditions, the hydrogen production experiments were carried out in an argon atmosphere. Before each experiment, the photocatalytic cell was purged with argon for 30 min to eliminate O_2.

Hydrogen gas evolution was measured by gas chromatography (Finnigan 9001) with thermal conductivity detection (TCD). Because He and H_2 have similar conductivity values, argon was used as a carrier gas. The separations were performed in a molecular sieve column (30 m × 0.32 mm × 12.00 μm). The GC oven temperature was set at 35 °C.

In a typical photolysis experiment, 60 mg of a target photocatalyst was dispersed in an aqueous solution (total volume = 60 mL) containing 30% glycerol and 40 μL of 8% H_2PtCl_6 (~0.3 wt.% Pt), with pH adjusted to 11 by the addition of a NaOH solution. Metallic platinum was deposited *in situ* on the photocatalyst surface by the photodecomposition of $PtCl_6^{2-}$. The photocatalytic cell was equipped with argon gas inlet/outlet tubes, which serve to collect and transfer gaseous products to the analytical system. Aliquots of three samples were injected at each time point to ensure precision. The photocatalytic reactions of each photocatalyst sample were performed in triplicate.

After 7 h of irradiation, a sample of liquid phase was collected, filtered and analyzed in a high performance liquid chromatography

system coupled to a UV/DAD detector system (HPLC/UV/DAD, Agilent 1100, with detection at 365 nm), after a derivatization reaction with a 2,4-dinitrophenylhydrazine (2,4-DNPH) solution to form the respective 2,4-dinitrophenylhydrazones [39,40]. The carbonyl compound derivatives were separated in an x-Terra MS column. Acetonitrile and water were used as the mobile phase according to the following procedure: 0–30 min from 40% to 100% acetonitrile, and 60% to 0% water. The flow rate was 0.250 mL min^{-1} and the injection volume was 10 μL.

3. Results and discussion

The X-ray diffraction patterns of bulk-phase hex-CdS (sample 1) and the hybrid materials, TiO_2/hex-CdS (sample 2) and CdS/TiO_2 (sample 3), which are shown in Fig. 1, confirm the presence of hex-CdS wurtzite structure (samples 1 and 2) and anatase TiO_2 phase (samples 2 and 3) by comparison with the ICSD patterns. However, sample 1 shows low intensity peaks associated with CdO contamination, which probably occurred during the heat treatment. The TiO_2/hex-CdS pattern (sample 2) shows peaks related to TiO_2, although they are poorly defined due to the small particle size. No peaks related to cubic or hexagonal CdS were identified in CdS/TiO_2 (sample 3) due to the very small amount of nanoparticles deposited on the bulk TiO_2.

Table 1
Band gap energy values of synthesized samples and commercial CdS, determined by the derivative method.

Material	Band gap energy/eV
Commercial CdS	2.26 ± 0.07
TiO_2/hex-CdS	2.33 ± 0.07
hex-CdS	2.40 ± 0.07
CdS/TiO_2	2.44 ± 0.07

Fig. 2 shows the visible PA spectra of the commercial CdS (a), hex-CdS (b), TiO_2/hex-CdS (c), and CdS/TiO_2 (d). The apparent band gap energies, E_g, of all the materials were determined from PA spectra data based on an evaluation of the absorption intensity derivative near the fundamental absorption edge [41,42]. The inflection point of the first derivative yields the E_g. Table 1 lists the corresponding band gap energies obtained. The determination of the energy gap shows a total error of about 3%. The precision of these results is due to the large number of statistics provided by

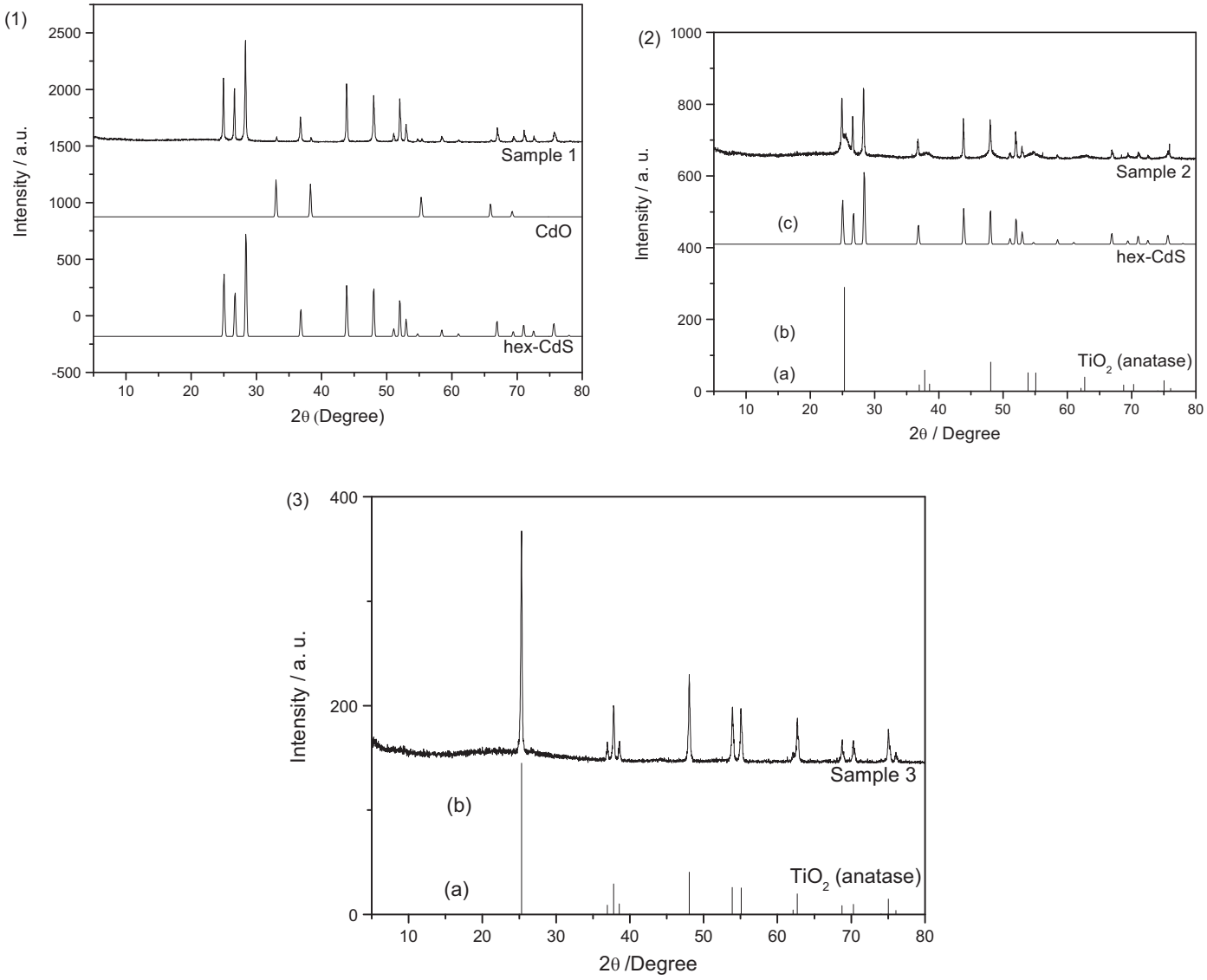

Fig. 1. XRD patterns of samples 1–3 and ICSD patterns for the phases CdS wurtzite (pdf # 01-075-1545-41-1049); TiO_2 anatase (pdf # 01-071-1166-21-1272) and CdO (pdf # 01-073-2245-5-640).

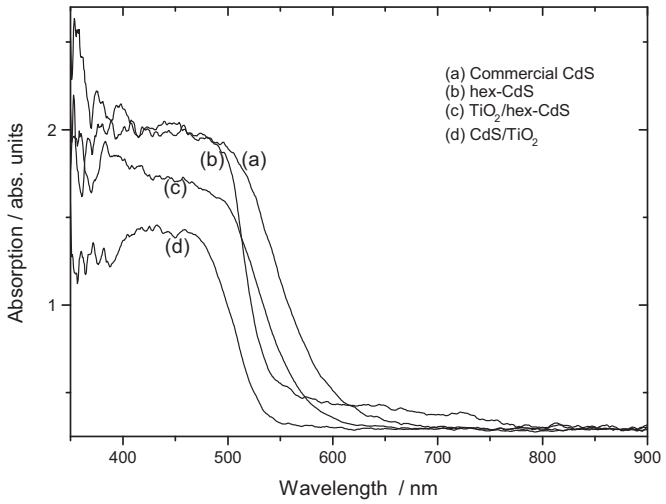

Fig. 2. Photoacoustic spectra of: (a) hex-CdS; (b) commercial CdS; (c) CdS/TiO_2; and (d) TiO_2/hex-CdS.

long-term measuring routines. Since TiO_2 does not absorb in the visible range, shifts in band gap energies are due to distinct specimens of CdS. The band gap of CdS employed in the TiO_2/hex-CdS hybrid photocatalyst is shifted in comparison to the pure hex-CdS, probably by an electronic semiconductor support interaction; while the deposition of CdS nanoparticles on bulk TiO_2, CdS/TiO_2, prevents the aggregation of CdS, resulting in small absorbing particles and a blue shift in the absorption spectrum.

The hydrogen production rate was measured from an aqueous solution containing glycerol (30%) as sacrificial reagent under visible light irradiation ($\lambda \geq 418$ nm). Fig. 3 shows the profile of hydrogen production as a function of time for each target photocatalyst. All the photocatalysts evaluated here exhibited photoactivity in hydrogen production when exposed to visible light. The kinetic curves display an apparent induction period of 0.5–1 h before the evolution of hydrogen started with the Pt/hex-CdS and $Pt/CdS/TiO_2$ photocatalysts. The Pt/TiO_2/hex-CdS photocatalyst did not show such an induction period. These results are in accordance those obtained by Jang et al. [35], who did not observe the induction period for Pt/TiO_2/hex-CdS when they used an aqueous solution containing sulfide and sulfite ions as sacrificial reagents. However, the induction periods for Pt/hex-CdS and $Pt/CdS/TiO_2$ were 1–2 h.

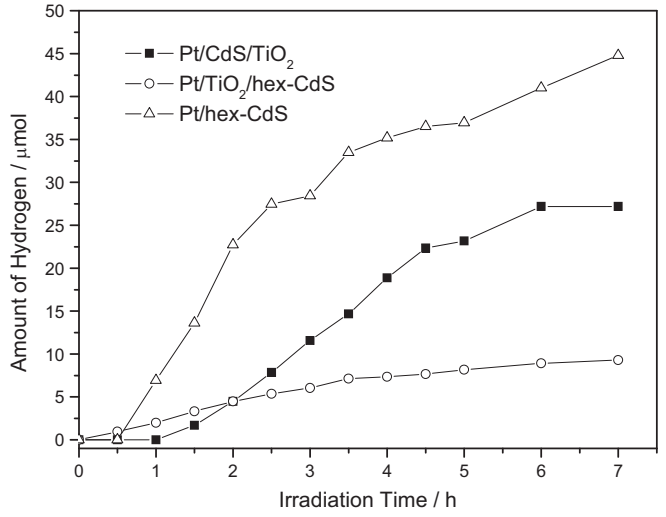

Fig. 3. Hydrogen production from different photocatalyst configurations: $Pt/CdS/TiO_2$, Pt/TiO_2/hex-CdS and Pt/hex-CdS.

Table 2
Rates of hydrogen evolution obtained from the photoreforming of glycerol under a visible solar light-simulating source, and comparison with other works that used UV light.

Photocatalyst	Radiation	H_2 production $\mu mol\ g_{cat}^{-1}\ h^{-1}$	Reference
0.3 wt.% Pt/TiO_2/hex-CdS	Visible	2.2×10^1	–
0.3 wt.% $Pt/CdS/TiO_2$	Visible	6.5×10^1	–
0.3 wt.% Pt/hex-CdS	Visible	1.07×10^2	–
0.5 wt.% Pt/TiO_2	UV	3.5×10^2	[31]
0.5 wt.% Pt/TiO_2	UV	4.35×10^2 (60 °C)	[32]
2.0 wt.% (B, N)-codoped TiO_2	UV	8.3×10^3	[43]

Under the present experimental conditions, the maximum hydrogen evolution rate achieved was 107 $\mu mol\ g_{cat}^{-1}\ h^{-1}$ when Pt/hex-CdS was irradiated using a solar light-simulating source in a visible light range, followed by $Pt/CdS/TiO_2$, which produced 65 $\mu mol\ g_{cat}^{-1}\ h^{-1}$. Our findings also indicated that TiO_2 does not increase the efficiency of hex-CdS in driving the photoinduced reforming of glycerol, since the hydrogen production rate remained as low as 22 $\mu mol\ g_{cat}^{-1}\ h^{-1}$ for Pt/TiO_2/hex-CdS.

Table 2 compares our results with hydrogen evolution rates obtained from the photoreforming of glycerol using a solar light-simulating source and modified TiO_2 as photocatalyst. Our results are comparable to those obtained by Kondarides et al. [31] and Daskalaki and Kondarides [32], but are still lower than those reported by Luo et al. [43], who used UV light irradiation.

Systems with CdS/aqueous solution interfacial contact showed better activities, suggesting that the hydrogen production mechanism can be influenced by hydrolytic surface reactions on CdS. The lower activity of $Pt/CdS/TiO_2$ may have been due to the fact that the potential conduction band (CB) edge of TiO_2 ($E_{CB} = -0.43$ V vs. NHE at pH 10) is more positive than that of CdS ($E_{CB} = -0.75$ V vs. NHE), creating the potential gradient at the CdS/TiO_2 interface. The CB electrons generated on CdS and trapped by platinum attached to the CdS surface are transferred to TiO_2 CB through the potential gradient. The same potential gradient is created in TiO_2/CdS, but in this case, the photogenerated holes on the CdS surface are less accessible to glycerol, resulting in the photocorrosion of the semiconductor.

Table 3 shows the results of the liquid phase analysis performed by HPLC after 7 h of irradiation, as well as the hydrogen accumulated during this period. The results demonstrate that the reaction proceeded with the production of intermediate products such as formaldehyde, acetaldehyde, acrolein and propanone. In general, the concentration of carbonyl compounds increases during the production of hydrogen, indicating that the CCs produced originate from the photoinduced reforming and the existence of parallel reaction pathways. It may be suggested that glycerol undergoes dehydrogenation steps on the metal surface to yield H_2 and adsorbed intermediates, and is followed by cleavage of C–C bonds and desorption of smaller molecules.

According to our previous studies [25], CdS reacts readily with water, giving rise hydrolyzed surface sites >Cd(II)SH and >CdOH

Table 3
Concentrations of remaining carbonyl compounds (CC) and hydrogen formed in the photolysis reaction after 7 h of irradiation.

Compound	Concentration ($\mu mol\ g_{cat}^{-1}$)		
	TiO_2/hex-CdS	CdS/TiO_2	hex-CdS
Formaldehyde	0.182	0.378	0.966
Acetaldehyde	0.049	0.063	0.175
Acrolein	0.112	0.028	0.231
Propanone	0.042	–	0.133
Hydrogen	155	453.3	746.7

that undergo several proton transfer reactions. Upon equilibration in water, CdS can be photoexcited to produce trapped electrons and holes at the various surface sites ($^{S^{2-}}_{Cd^{2+}}>Cd(+I)S(-I)H$ and $^{S^{2-}}_{Cd^{2+}}>Cd(0)S(0)H$). The trapped photogenerated electrons are used to reduce protons toward molecular hydrogen, as follows:

$$^{S^{2-}}_{Cd^{2+}}>Cd(0)S(0)H + H^+ \rightarrow {}^{S^{2-}}_{Cd^{2+}}>Cd(0)S(0)H_2^+ \rightarrow {}^{S^{2-}}_{Cd^{2+}}>Cd(?\,II)S(0)^+ + H_2 \quad (2)$$

However, the major hydrogen is generated on platinum surface. Bowker et al. [44] proposed a mechanism for photocatalytic glycerol reforming reaction on Pd/TiO_2 based on glycerol decomposition to gas phase hydrogen, an organic moiety and adsorbed CO on the metal as the initiation of the process. According to this proposition, the reaction stops after very little hydrogen has evolved due to blockage of the surface with CO, which is strongly held and has a self-poisoning. Adsorbed CO was, than, removed as CO_2 by an active oxygen species. In our case, we detected induction periods for Pt/hex-CdS and $Pt/CdS/TiO_2$ photocatalysts, which could be an evidence of CO adsorbed on Pt. In this way, it is reasonable to believe that the glycerol reforming reaction on Pt/hex-CdS and $Pt/CdS/TiO_2$ follows a similar mechanism. Meanwhile, the active oxygen species responsible for CO removing are not come from semiconductor surface, since the interfacial contact in two cases is CdS/solution instead TiO_2/solution. Probably, these species are formed after reaction of water with holes to yield hydrogen peroxide and hydroxyl radicals on semiconductor surface, which can combine with CO as follows:

$$CO + H_2O_2 \rightarrow CO_2 + H_2O \quad (3)$$

$$CO + OH^{\cdot} + h^+ \rightarrow CO_2 + H^+ \quad (4)$$

Another possible mechanism for glycerol photooxidation can be proposed taking into account the carbonyl compounds identified in the liquid phase. If glycerol oxidation is initiated at surface-trapped holes (e.g., $^{S^{2-}}_{Cd^{2+}}>Cd(+II)S(0)^+$) via primary carbon, glyceraldehyde can be formed as an intermediary product, leading to the formation of acrolein as the main oxidation product, according to the proposed mechanism:

$$^{S^{2-}}_{Cd^{2+}}>Cd(+II)S(0)^+ + H_2COHCHOHCH_2OH \rightarrow {}^{S^{2-}}_{Cd^{2+}}>Cd(+II)S(-I)H^+ + H_2COHCHOH\dot{C}HOH \quad (5)$$

$$^{S^{2-}}_{Cd^{2+}}>Cd(+II)S(-I)H^+ + H_2COHCHOHCH_2OH \rightarrow {}^{S^{2-}}_{Cd^{2+}}>Cd(+II)S(-II)H_2^+ + H_2COHCHOH\dot{C}HOH \quad (6)$$

$$2H_2COHCHOH\dot{C}HOH \rightarrow 2H_2COHCHOHCHO + H_2 \quad (7)$$

$$H_2COHCHOHCHO + {}^{S^{2-}}_{Cd^{2+}}>Cd(+II)S(-II)H_2^+ \rightarrow H_2C=CHCHO + 2H_2O + {}^{S^{2-}}_{Cd^{2+}}>Cd(+II)S(0)^+ \quad (8)$$

All the photolysis reactions were carried out at pH 11. At high pH, the $^{S^{2-}}_{Cd^{2+}}>CdOH$ surface site may play an important role in the initial steps of proton reduction (a proton bound to O^{2-}) on the surface of CdS [25], as follows:

$$^{S^{2-}}_{Cd^{2+}}>CdOH \xrightarrow{h^+_{VB}} {}^{S^{2-}}_{Cd^{2+}}>CdOH^+ \xrightarrow{H_2COHCHOHCH_2OH} {}^{S^{2-}}_{Cd^{2+}}>CdOH_2^+ + H_2COHCHOH\dot{C}HOH \quad (9)$$

$$^{S^{2-}}_{Cd^{2+}}>CdOH_2^+ \xrightarrow{2e^-_{CB}} {}^{S^{2-}}_{Cd^{2+}}>CdO^- + H_2 \quad (10)$$

Otherwise, if glycerol oxidation is initiated at surface-trapped holes via secondary carbon, the intermediary product may be 1,3-dihidroxi-2-propanone instead of glyceraldehyde, which is involved in subsequent redox reactions to yield propanone as the main product, following a mechanism similar to that described above. Since the concentrations of remaining carbonyl compounds identified were extremely low compared to the hydrogen accumulated in 7 h of irradiation (Table 3), these compounds, as well as fragments adsorbed on the photocatalyst surface, such as formaldehyde and acetaldehyde, were oxidized sequentially by photogenerated oxidants toward CO_2.

4. Conclusions

The photocatalytic reforming of aqueous biomass solutions could be an interesting and innovative route to produce hydrogen in ambient conditions. The samples tested here exhibited an unprecedented activity in the photoinduced reforming of biomass under visible light irradiation, particularly the samples with CdS/aqueous solution interfacial contact. Our results open up prospects for improving systems that are able to drive photoinduced reforming with visible light illumination to make effective use of solar light and produce hydrogen from glycerol, a renewable raw material.

Acknowledgements

The authors acknowledge the Brazilian research funding agency CNPq for its financial support of this research.

References

[1] A.C. Pinto, L.L.N. Guarieiro, M.J.C. Rezende, N.M. Ribeiro, E.A. Torres, W.A. Lopes, P.A.P. Pereira, J.B. de Andrade, J. Braz, Chem. Soc. 16 (2005) 1313.
[2] R. Hashaikeh, I.S. Butler, J.A. Kozinski, Energy Fuels 20 (2006) 2743.
[3] S. Authayanun, A. Arpornwichanop, W. Paengjuntuek, S. Assabumrungrat, Int. J. Hydrogen Energy 35 (2010) 6617.
[4] G. Wena, Y. Xu, H. Ma, Z. Xu, Z. Tian, Int. J. Hydrogen Energy 33 (2008) 6657.
[5] A.T. Marshall, R.G. Haverkamp, Int. J. Hydrogen Energy 33 (2008) 4649.
[6] G. Sabourin-Provost, P.C. Hallenbeck, Bioresour. Technol. 100 (2009) 3513.
[7] A.J. Byrd, K.K. Pant, R.B. Gupta, Fuel 87 (2008) 2956.
[8] S. Adhikari, S. Fernando, S.R. Gwaltney, S.D.F. To, R.M. Bricka, P.H. Steele, A. Haryanto, Int. J. Hydrogen Energy 32 (2007) 2875.
[9] M.R. Hoffmann, S.T. Martin, W. Choi, D.W. Bahnemann, Chem. Rev. 95 (1995) 69.
[10] C. Wang, R. Pagel, J.K. Dohrmann, D.W. Bahnemann, C.R. Chimie 9 (2006) 761.
[11] A.J. Bard, J. Photochem. 10 (1979) 59.
[12] A.J. Nozik, J. Phys. Chem. 100 (1996) 13061.
[13] M. Grätzel, Nature 414 (2001) 338.
[14] K. Maeda, K. Domen, J. Phys. Chem. C 111 (2007) 7851.
[15] A. Kudo, Int. J. Hydrogen Energy 31 (2006) 197.
[16] M. Matsuoka, M. Kitano, M. Takeuchi, K. Tsujimaru, M. Anpo, J.M. Thomas, Catal. Today 122 (2007) 51.
[17] A. Fujishima, K. Honda, Nature 238 (1972) 37.
[18] A. Fujishima, X. Zhang, D.A. Tryk, Int. J. Hydrogen Energy 32 (2007) 2664.
[19] M. Antoniadou, D.I. Kondarides, D. Labou, S. Neophytides, P. Lianos, Sol. Energy Mater. Solar Cells 94 (2010) 592.
[20] D. Bahnemann, Sol. Energy 77 (2004) 445.
[21] J. Zhao, X.D. Yang, Building Environ. 38 (2003) 645.
[22] M.C. Canela, W.F. Jardim, Environ. Technol. 29 (2008) 673.
[23] P. Peralta-Zamora, E. Espósito, J. Reyes, N. Duran, Quim. Nova 20 (1997) 186.
[24] X. Fu, J. Long, X. Wang, D.Y.C. Leung, Z. Ding, L. Wu, Z. Zhang, Z. Li, X. Fu, Int. J. Hydrogen Energy 33 (2008) 6484.
[25] L.A. Silva, S.Y. Ryu, J. Choi, W. Choi, M.R. Hoffmann, J. Phys. Chem. C 112 (2008) 12069.
[26] H.A.J.L. Mourão, V.R. Mendonça, A.R. Malagutti, C. Ribeiro, Quim. Nova 32 (2009) 2181.
[27] A. Patsoura, D.I. Kondarides, X.E. Verykios, Appl. Catal. B 64 (2006) 171.
[28] A. Patsoura, D.I. Kondarides, X.E. Verykios, Catal. Today 124 (2007) 94.
[29] N. Strataki, V. Bekiari, D.I. Kondarides, P. Lianos, Appl. Catal. B 77 (2007) 184.
[30] T. Kawai, T. Sakata, Chem. Lett. 10 (1981) 81.
[31] D.I. Kondarides, V.M. Daskalaki, A. Patsoura, X.E. Verykios, Catal. Lett. 122 (2008) 26.
[32] V.M. Daskalaki, D.I. Kondarides, Catal. Today 144 (2009) 75.
[33] J. Choi, S.Y. Ryu, W. Balcerski, T.K. Lee, M.R. Hoffmann, J. Mater. Chem. 18 (2008) 2371.
[34] M. Matsumura, S. Furukawa, Y. Saho, H. Tsubomura, J. Phys. Chem. 89 (1985) 1327.
[35] J.S. Jang, W. Li, S.H. Oh, J.S. Lee, Chem. Phys. Lett. 425 (2006) 278.
[36] J.S. Jang, S.M. Ji, S.W. Bae, H.C. Son, J.S. Lee, J. Photochem. Photobiol. A: Chem. 188 (2007) 112.
[37] H. Park, W. Choi, M.R. Hoffmann, J. Mater. Chem. 18 (2008) 2379.
[38] Y. Bessekhouad, D. Robert, J.V. Weber, J. Photochem. Photobiol. A: Chem. 163 (2004) 569–580.
[39] L.C. de Azevedo, M.M. Reis, L.F. Motta, G.O. da Rocha, L.A. Silva, J.B. de Andrade, J. Agric. Food Chem. 55 (2007) 8670.
[40] L.C. de Azevedo, M.M. Reis, G.E. Pereira, G.O. da Rocha, L.A. Silva, J.B. de Andrade, J. Sep. Sci. 32 (2009) 3432.
[41] L.A. Silva, M.A. de Araujo, J.B. de Andrade, K.A. Silva, D.G.F. David, A. Ferreira da Silva, I. Pepe, Chem. Phys. Lett. 442 (2007) 84.
[42] T.B.F. Guimarães, I. Pepe, A. Ferreira da Silva, A.S. Mangrich, J.B. de Andrade, L.A. Silva, J. Alloys Compd. 481 (2009) 654.
[43] N. Luo, Z. Jiang, H. Shi, F. Cao, T. Xiao, P.P. Edward, Int. J. Hydrogen Energy 34 (2009) 125.
[44] M. Bowker, P.R. Davies, L.S. Al-Mazroai, Catal Lett. 128 (2009) 253.